

Metal Nanocrystals

Size- and Shape-Selective Synthesis of Metal Nanocrystals and Nanowires Using CO as a Reducing Agent**

Yijin Kang, Xingchen Ye, and Christopher B. Murray*

Colloidal metal nanocrystals (NCs) have been extensively studied because of their various applications in catalysis,^[1,2] sensors,^[3,4] surface-enhanced spectroscopy,^[5] and biological imaging.^[6] A variety of wet chemical approaches have been developed to prepare both monodisperse spherical^[7,8] and nonspherical^[9–14] metal NCs; the latter often exhibit properties unobtainable simply by tuning the size of the spheres. The synthesis of metal NCs typically employs the reduction or decomposition of metal precursors in the presence of ligands, which prevent aggregation and improve the colloidal stability of the NCs. Among the wide spectrum of reducing agents that have been used, gases such as hydrogen under pressure have proven effective in delicately manipulating the growth kinetics and thus tailoring the size and morphology of the metal NCs.^[15,16] Despite these efforts, a one-pot synthesis of highly monodisperse metal NCs at ambient pressure using gaseous reducing agents generated at point-of-use is still an important advance.

Herein we report the size- and shape-selective formation of metal nanostructures including Pt nanocubes, Pd spherical NCs, and Au nanowires (NWs) using carbon monoxide (CO, generated at point-of-use) as a reducing agent. We also discuss the implications of our observation on several recent reports of the preparation of PtNCs utilizing metal carbonyls.

In catalysis, it is well-known that particle shape (the facets exposed) can be as important as the particle surface area in activity and selectivity. For example, Pt(100) exhibits higher electrocatalytic activity than Pt(111) for the oxygen reduction reaction in H₂SO₄ electrolyte.^[17,18] Pt(100) also shows different selectivity from Pt(111) towards hydrogenation reactions.^[19] Thus Pt nanocubes with well-defined {100} facets provide a model system for understanding microscopic surface phenomena in many catalytic processes. We report the synthesis of Pt nanocubes employing CO (generated by dehydration of formic acid; Supporting Information, Fig-

ure S1) as a mild reducing agent. Pt nanocubes with straight edges (edge length = 8.9 nm, $\sigma = 6\%$) and sharp corners are produced after 15 min of reaction at 200 °C (Figure 1). The X-

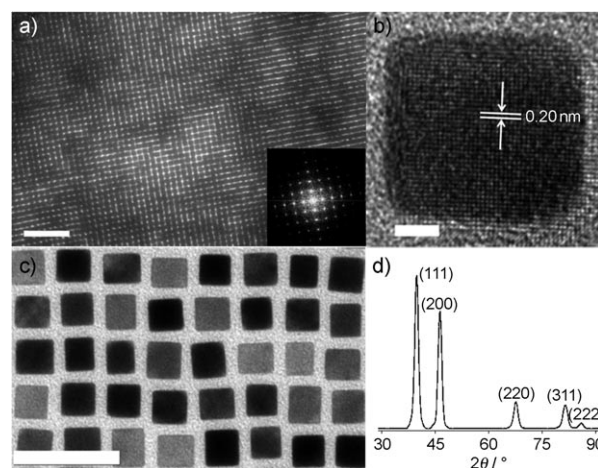


Figure 1. a, c) TEM images, b) HRTEM image, and d) XRD pattern of Pt nanocubes synthesized using gaseous CO. Inset in (a): fast-Fourier-transform pattern of the self-assembled Pt nanocube superlattices with simple cubic symmetry. Scale bars: a) 100 nm, b) 2 nm, c) 30 nm.

ray diffraction (XRD) pattern (Figure 1d) of the as-synthesized Pt nanocubes confirms the face-centered cubic (fcc) crystal structure. High-resolution TEM (HRTEM) image of a single Pt nanocube reveals an interplanar distance of about 0.20 nm, which is consistent with the lattice spacing of the {100} planes of the fcc platinum structure (Figure 1b). Furthermore, study of the shape evolution (Figure 2) reveals that NCs formed at the early stage (2–4 min) of the reaction typically adopt a polyhedral shape. As the reaction proceeds, the particles transform to cubes. The reaction exhibits a minimum size- and shape dispersity at about 15 min, after which the size distribution broadens and other shapes (rods, truncated cubes, and polyhedra) start to appear. To confirm the role of CO as a reducing agent, the following control experiments were performed: the reaction mixture was bubbled with CO for 10 min at room temperature and then purged with N₂ for 20 min. After that, the solution was brought to 200 °C and kept at this temperature for 15 min. This process only produces large aggregates of irregular shaped NCs (Supporting Information, Figure S2c), similar to the products synthesized in the absence of CO (Supporting Information, Figure S2a,b). This observation implies that in the present case, CO neither serves as ligand nor forms complex with platinum, which is different in mechanism from

[*] Y. Kang,^[†] X. Ye,^[†] Prof. C. B. Murray
Department of Chemistry, University of Pennsylvania
Philadelphia, PA 19104 (USA)
E-mail: cbmurray@sas.upenn.edu

Prof. C. B. Murray
Department of Materials Science and Engineering
University of Pennsylvania (USA)

[†] These authors contributed equally to this work.

[**] The synthesis of PtMn nanocrystal magnets was developed with partial support from the Army Research Office through MURI Award W911NF-08-1-0364 (Y.K.), while studies of plasmonic gold nanowires were funded by the Department of Energy's Division of Basic Energy Sciences through Award: DE-SC0002158 (X.Y. & C.B.M.).

Supporting information for this article is available on the WWW under <http://dx.doi.org/10.1002/anie.201003383>.

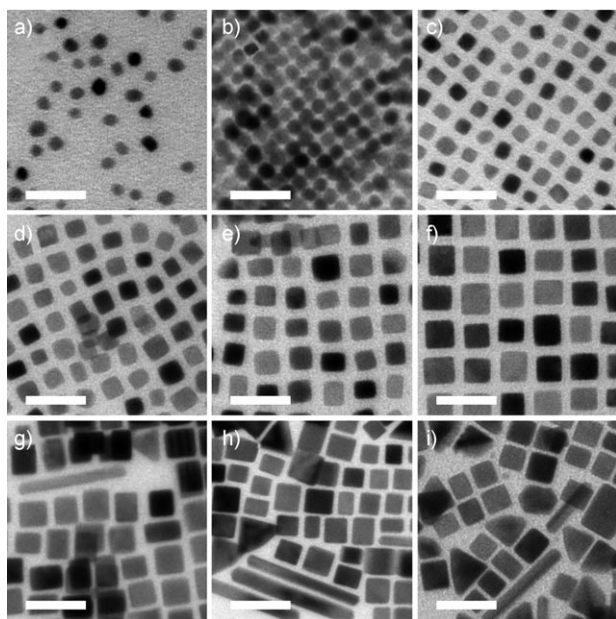


Figure 2. TEM images taken at different stages of Pt nanocube syntheses using CO. a) 2 min, b) 4 min, c) 6 min, d) 8 min, e) 10 min, f) 15 min, g) 20 min, h) 30 min, i) 90 min. Scale bars: 20 nm.

previous studies using $[\text{Pt}(\text{dba})_2]$ precursors (dba = dibenzylideneacetone).^[20,21] Furthermore, the FTIR spectra (Supporting Information, Figure S3) of the Pt nanocubes show no peaks in the region of $1800\text{--}2300\text{ cm}^{-1}$, suggesting that there is no Pt–CO species in the products.

Recently we synthesized MnPt nanocubes with a composition of Mn/Pt $\approx 1:3$.^[22] However, by reducing the amount of $[\text{Mn}_2(\text{CO})_{10}]$, uniform Pt nanocubes ($>99.0\%$ Pt content by elemental analyses) can be produced rather than the MnPt nanocubes (Supporting Information, Figure S5). Sun et al. have reported the synthesis of Pt nanocubes by using $[\text{Fe}(\text{CO})_5]$, demonstrating that the presence of $[\text{Fe}(\text{CO})_5]$ facilitates the nucleation and controls the growth of Pt nanocubes.^[23] Several subsequent reports also focus on the synthesis of Pt nanocubes employing metal carbonyls.^[24,25] Some researchers claim that the metal (W, Co) decomposed from carbonyl compounds plays the key role (serving as the nucleation center or as the in-situ-generated reducing agent) during the synthesis of Pt nanocubes. However, based on our observations, the presence of neither foreign metals (W, Co) nor metal carbonyls are necessary for the growth of uniform Pt nanocubes. Furthermore, metal carbonyls can introduce impurities either as alloy incorporated into Pt or as adatoms on Pt surfaces, which could result in surface properties distinct from those of “clean” Pt NCs.^[26] In contrast, CO-assisted synthesis produces Pt nanocubes with high chemical purity, crystallinity, and shape uniformity.

In recognition of the fact that foreign metals (Fe, W, Co, etc.) are not essential for the formation of well-faceted metal NCs, we extended the synthetic use of CO as a reducing agent to other metal NCs. Palladium is widely used as catalysts in catalytic converters^[27] and in a range of organic reactions, including cross-coupling reactions^[28] and hydrogenation.^[29] Several research groups have also demonstrated the use of

PdNCs as primary catalysts or a co-catalyst for fuel-cell applications, with enhanced performance and greater stability compared to pure Pt catalysts.^[1,30–32] Despite the recent advances in the shape-controlled synthesis of Pd nanostructures,^[33] one-pot synthesis of monodisperse spherical PdNCs has been limited. Importantly, previous studies showed that trioctylphosphine (TOP) can serve as an effective ligand in the synthesis of monodisperse PdNCs.^[34] Herein we demonstrate that by using the Pd–TOP precursor, monodisperse PdNCs can be produced under a CO blanket within 10 min at 195°C . TEM images (Figure 3 a,b) show that 5.8 nm PdNCs

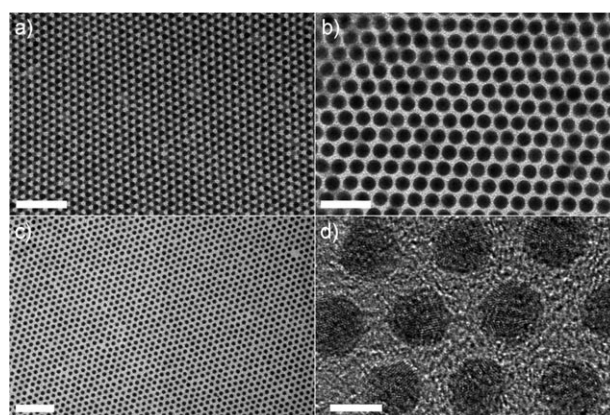


Figure 3. TEM images of a,b) 5.8 nm and c) 5.0 nm PdNCs. d) HRTEM image of the 5.8 nm PdNCs. Scale bars: a,c) 50 nm, b) 20 nm, d) 5 nm.

self-assemble into close-packed superlattices. A HRTEM image of the 5.8 nm PdNCs reveals that most NCs are twinned, which is commonly seen in small metal NCs (Figure 3d). Transmission small-angle X-ray scattering (TSAXS) pattern (Supporting Information, Figure S11) of the 5.8 nm PdNCs is fitted to the spherical model with a diameter of 6.05 nm and a size distribution of about 9%, which is consistent with the TEM and HRTEM observations. The powder XRD pattern confirms the fcc crystal structure (Supporting Information, Figure S6). By changing the reaction medium from a mixture of oleic acid and oleylamine to trioctylamine, 5.0 nm PdNCs are produced (Figure 3c).

Recognizing the potential of CO to accelerate reaction rates, we target the use of CO to the synthesis of ultrathin AuNWs. Several groups have developed colloidal methods to synthesize uniform AuNWs. However, these recipes usually require hours or even days.^[35–38] As a final example, we demonstrate that the ultrathin AuNWs can be synthesized within 10 min by reducing AuCl–oleylamine complexes with CO. The AuNWs form within 2 min after introducing CO, growing longer as the reaction proceeds (Supporting Information, Figure S14). TEM images of different magnifications show that the AuNWs obtained tend to assemble into bundles (Figure 4; Supporting Information, Figures S12, S13). Individual AuNWs typically terminates with enlarged spherical ends (Figure 4c). Similar wires have been observed and proposed to result from oriented attachment during the growth.^[39] The AuNWs are of about 2.5 nm in width and of

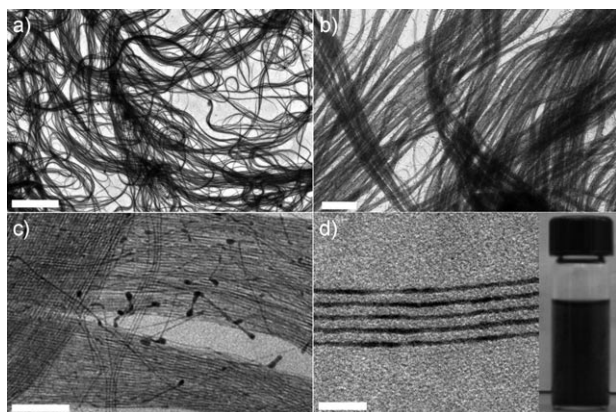


Figure 4. TEM images of ultrathin Au nanowires. Inset in (d): photograph of Au nanowires dispersed in hexane. Scale bars: a) 5 μm , b) 0.5 μm , c) 100 nm, d) 20 nm.

several micrometers in length (Figure 4d). Furthermore, ultrathin AuNWs can also be produced with AuCl_3 , albeit in lower yield (Supporting Information, Figure S17). These one-dimensional metal nanostructures are promising building blocks for plasmonic waveguides^[40] and nano-electronic devices.^[41]

In summary, we have developed a general approach for the shape-selective synthesis of different metal NCs and AuNWs with a narrow size distribution. The use of CO was found to play an important role in controlling the reaction kinetics and the morphology of the metal nanostructures. These synthetic routes are being extended to the design of other colloidal metal and metal alloy NCs.

Experimental Section

Gaseous CO was generated at point-of-use by dehydration of formic acid. Briefly, formic acid was delivered into warm concentrated sulfuric acid (60 °C) at a constant rate using syringe pump (Caution: CO is toxic and all operations should be carried out inside a well-ventilated hood!). All syntheses were performed using standard Schlenk techniques.

Synthesis of Pt nanocubes: $[\text{Pt}(\text{acac})_2]$ (0.04 g) was dissolved in benzyl ether (5 mL), oleylamine (3.68 mL), and oleic acid (0.63 mL) under an N_2 atmosphere. Gaseous CO was then introduced to the solution (ca. $10 \text{ cm}^3 \text{ min}^{-1}$) at room temperature. The reaction flask was then placed into a preheated oil bath. After 15 min of reaction at 200 °C, the solution was allowed to cool and the products were isolated by adding ethanol and centrifugation. The NCs were then redispersed in hexane.

Synthesis of Pd spherical NCs: The Pd-TOP complex was prepared by dissolving $[\text{Pd}(\text{acac})_2]$ (0.05 g) in TOP (0.6 mL). The resulting precursor was mixed with TOP (0.15 mL), oleic acid (2 mL), and oleylamine (13 mL) at room temperature. Under a constant heating rate of $15^\circ\text{C min}^{-1}$, the solution was brought to 195 °C, at which point CO was introduced to the reaction flask (ca. $15 \text{ cm}^3 \text{ min}^{-1}$). The reaction was conducted for 10 min and the products were purified as described above.

Synthesis of AuNWs: AuCl_3 (0.046 g) was dissolved in chloroform (20 mL) and oleylamine (1.84 mL). The mixture was then heated to 60 °C and CO was introduced to the reaction flask (ca. $15 \text{ cm}^3 \text{ min}^{-1}$). After 10 min, the solution was allowed to cool to room temperature

and was diluted with hexane. The NWs were precipitated by centrifugation at 6000 rpm.

Characterization: Transmission electron microscopy (TEM) was carried out with a JEOL1400 operating at 120 kV. High-resolution TEM (HRTEM) images and energy dispersive X-ray spectra (EDX) were obtained with a JEOL2010F (200 kV). X-ray diffraction (XRD) and transmission small-angle X-ray scattering (TSAXS) patterns were obtained on Rigaku Smartlab diffractometer with $\text{Cu}_{K\alpha}$ radiation ($\lambda = 1.5418 \text{ \AA}$). For TSAXS measurement, a hexane solution of PdNCs was loaded into a capillary tube. The TSAXS pattern was fitted using NANO-Solver (Rigaku software). Quantitative elemental analyses were carried out with both EDX and inductively coupled plasma optical emission spectrometry (ICP-OES) on SPECTRO GENESIS ICP spectrometer.

Received: June 3, 2010

Published online: July 26, 2010

Keywords: carbon monoxide · gold · nanocrystals · palladium · platinum

- [1] B. Lim, M. J. Jiang, P. H. C. Camargo, E. C. Cho, J. Tao, X. M. Lu, Y. M. Zhu, Y. N. Xia, *Science* **2009**, *324*, 1302.
- [2] S. E. Habas, H. Lee, V. Radmilovic, G. A. Somorjai, P. Yang, *Nat. Mater.* **2007**, *6*, 692.
- [3] S. J. Park, T. A. Taton, C. A. Mirkin, *Science* **2002**, *295*, 1503.
- [4] A. J. Haes, R. P. Van Duyne, *J. Am. Chem. Soc.* **2002**, *124*, 10596.
- [5] A. Tao, F. Kim, C. Hess, J. Goldberger, R. R. He, Y. G. Sun, Y. N. Xia, P. D. Yang, *Nano Lett.* **2003**, *3*, 1229.
- [6] M. S. Yavuz, Y. Y. Cheng, J. Y. Chen, C. M. Copley, Q. Zhang, M. Rycenga, J. W. Xie, C. Kim, K. H. Song, A. G. Schwartz, L. H. V. Wang, Y. N. Xia, *Nat. Mater.* **2009**, *8*, 935.
- [7] S. Stoeva, K. J. Klabunde, C. M. Sorensen, I. Dragieva, *J. Am. Chem. Soc.* **2002**, *124*, 2305.
- [8] N. F. Zheng, G. D. Stucky, *J. Am. Chem. Soc.* **2006**, *128*, 14278.
- [9] Y. G. Sun, Y. N. Xia, *Science* **2002**, *298*, 2176.
- [10] R. C. Jin, Y. W. Cao, C. A. Mirkin, K. L. Kelly, G. C. Schatz, J. G. Zheng, *Science* **2001**, *294*, 1901.
- [11] N. R. Jana, L. Gearheart, C. J. Murphy, *J. Phys. Chem. B* **2001**, *105*, 4065.
- [12] C. J. Murphy, T. K. Sau, A. M. Gole, C. J. Orendorff, J. X. Gao, L. Gou, S. E. Hunyadi, T. Li, *J. Phys. Chem. B* **2005**, *109*, 13857.
- [13] J. Perez-Juste, I. Pastoriza-Santos, L. M. Liz-Marzan, P. Mulvaney, *Coord. Chem. Rev.* **2005**, *249*, 1870.
- [14] T. K. Sau, A. L. Rogach, *Adv. Mater.* **2010**, *22*, 1781.
- [15] F. Dumestre, B. Chaudret, C. Amiens, P. Renaud, P. Fejes, *Science* **2004**, *303*, 821.
- [16] J. T. Ren, R. D. Tilley, *J. Am. Chem. Soc.* **2007**, *129*, 3287.
- [17] N. M. Markovic, H. A. Gasteiger, P. N. Ross, *J. Phys. Chem.* **1995**, *99*, 3411.
- [18] C. Wang, H. Daimon, T. Onodera, T. Koda, S. H. Sun, *Angew. Chem.* **2008**, *120*, 3644; *Angew. Chem. Int. Ed.* **2008**, *47*, 3588.
- [19] K. M. Bratlie, H. Lee, K. Komvopoulos, P. D. Yang, G. A. Somorjai, *Nano Lett.* **2007**, *7*, 3097.
- [20] A. Rodriguez, C. Amiens, B. Chaudret, M. J. Casanove, P. Lecante, J. S. Bradley, *Chem. Mater.* **1996**, *8*, 1978.
- [21] C. Amiens, D. Decaro, B. Chaudret, J. S. Bradley, R. Mazel, C. Roucau, *J. Am. Chem. Soc.* **1993**, *115*, 11638.
- [22] Y. J. Kang, C. B. Murray, *J. Am. Chem. Soc.* **2010**, *132*, 7568.
- [23] C. Wang, H. Daimon, Y. Lee, J. Kim, S. Sun, *J. Am. Chem. Soc.* **2007**, *129*, 6974.
- [24] J. Zhang, J. Y. Fang, *J. Am. Chem. Soc.* **2009**, *131*, 18543.
- [25] S. I. Lim, I. Ojea-Jimenez, M. Varon, E. Casals, J. Arbiol, V. Puntès, *Nano Lett.* **2010**, *10*, 964.
- [26] M. E. Grass, Y. Yue, S. E. Habas, R. M. Rioux, C. I. Teall, P. Yang, G. A. Somorjai, *J. Phys. Chem. C* **2008**, *112*, 4797.

- [27] Y. Nishihata, J. Mizuki, T. Akao, H. Tanaka, M. Uenishi, M. Kimura, T. Okamoto, N. Hamada, *Nature* **2002**, *418*, 164.
- [28] S. W. Kim, M. Kim, W. Y. Lee, T. Hyeon, *J. Am. Chem. Soc.* **2002**, *124*, 7642.
- [29] M. Q. Zhao, R. M. Crooks, *Angew. Chem.* **1999**, *111*, 375; *Angew. Chem. Int. Ed.* **1999**, *38*, 364.
- [30] H. J. Lee, S. E. Habas, G. A. Somorjai, P. D. Yang, *J. Am. Chem. Soc.* **2008**, *130*, 5406.
- [31] Z. M. Peng, H. Yang, *J. Am. Chem. Soc.* **2009**, *131*, 7542.
- [32] C. Bianchini, P. K. Shen, *Chem. Rev.* **2009**, *109*, 4183.
- [33] Y. J. Xiong, Y. N. Xia, *Adv. Mater.* **2007**, *19*, 3385.
- [34] S. W. Kim, J. Park, Y. Jang, Y. Chung, S. Hwang, T. Hyeon, Y. W. Kim, *Nano Lett.* **2003**, *3*, 1289.
- [35] Z. Y. Huo, C. K. Tsung, W. Y. Huang, X. F. Zhang, P. D. Yang, *Nano Lett.* **2008**, *8*, 2041.
- [36] X. M. Lu, M. S. Yavuz, H. Y. Tuan, B. A. Korgel, Y. N. Xia, *J. Am. Chem. Soc.* **2008**, *130*, 8900.
- [37] C. Wang, Y. J. Hu, C. M. Lieber, S. H. Sun, *J. Am. Chem. Soc.* **2008**, *130*, 8902.
- [38] N. Pazos-Perez, D. Baranov, S. Irsen, M. Hilgendorff, L. M. Liz-Marzan, M. Giersig, *Langmuir* **2008**, *24*, 9855.
- [39] H. J. Feng, Y. M. Yang, Y. M. You, G. P. Li, J. Guo, T. Yu, Z. X. Shen, T. Wu, B. G. Xing, *Chem. Commun.* **2009**, 1984.
- [40] A. L. Pyayt, B. Wiley, Y. N. Xia, A. Chen, L. Dalton, *Nat. Nanotechnol.* **2008**, *3*, 660.
- [41] Y. Lu, J. Y. Huang, C. Wang, S. Sun, J. Lou, *Nat. Nanotechnol.* **2010**, *5*, 218.